

DETC2000/MECH-14129

MANIPULATOR CALIBRATION USING A SINGLE ENDPOINT CONTACT CONSTRAINT

Marco A. Meggiolaro¹

Massachusetts Institute of Technology
Department of Mechanical Engineering
77 Massachusetts Ave, Cambridge, MA 02139
USA, Tel 617-253-5095, Fax 617-258-7881

Guglielmo Scriffignano

Politecnico di Milano
Dipartimento di Meccanica
V. Bonardi, 9, 20133 Milano, Italy
Tel 02-2399-4720, Fax 02-7063-8377

Steven Dubowsky²

Massachusetts Institute of Technology
Department of Mechanical Engineering
77 Massachusetts Ave, Cambridge, MA 02139
USA, Tel 617-253-2144, Fax 617-258-7881

ABSTRACT

Most manipulator calibration techniques require expensive and/or complicated pose measuring devices, such as theodolites. This paper investigates a calibration method where the manipulator endpoint is constrained to a single contact point and executes self-motions. From the easily measured joint angle readings, and an identification model, the manipulator is calibrated. Adding a wrist force sensor allows for the calibration of elastic effects due to end-point forces and moments. Optimization of the procedure is discussed. Experimental results are presented, showing the effectiveness of the method.

INTRODUCTION

Physical errors, such as machining tolerances, assembly errors and elastic deformations, cause the geometric properties of a manipulator to be different from their ideal values. Model based error compensation of a robotic manipulator, also known as robot calibration, is a process to improve manipulator position accuracy using software. Classical calibration involves identifying an accurate functional relationship between the joint transducer readings and the workspace position of the end-effector in terms of parameters called generalized errors (Roth et al., 1987). This relationship is found from measured data and used to predict, and compensate for, the endpoint errors as a function of configuration.

Considerable research has been performed to make manipulator calibration more effective both in terms of required number of measurements and computation by the procedure (Hollerbach, 1988; Hollerbach and Wampler, 1996; Roth et al.,

1987). Several calibration techniques have been used to improve robot accuracy (Roth et al., 1987), including open and closed-loop methods (Everett and Lin, 1988). Open-loop methods require an external metrology system to measure the end-effector pose, such as theodolites. Obtaining open-loop measurements is generally very costly and time consuming, and must be performed regularly for very high precision systems. In contrast, closed-loop methods only need joint angle sensing, and the robot becomes self-calibrating. In closed-loop calibration, constraints are imposed on the end-effector of the robot, and the kinematic loop closure equations are adequate to calibrate the manipulator from joint readings alone. Past closed-loop methods have had the robot moving along an unsensed sliding joint at the endpoint, or constraining the end-effector to lie on a plane (Ikits and Hollerbach, 1997; Zhuang et al., 1999).

This paper investigates a closed-loop calibration method that was among a number suggested by (Bennett and Hollerbach, 1991). In the method, called here Single Endpoint Contact (SEC) calibration, the robot endpoint is constrained to a single contact point. Using an end-effector fixture equivalent to a ball joint, the robot executes self-motions to move to different configurations. At each configuration, manipulator joint sensors provide data that is used in an SEC identification algorithm to estimate the robot's parameters. A total least squares optimization procedure is used to improve the calibration accuracy (Hollerbach and Wampler, 1996).

In addition to geometric errors, this calibration method is able to identify elastic structural deformation errors due to task loads and gravity, since arbitrary forces can be applied to the

¹ASME Student Member

²ASME Fellow

SEC fixture. The error model is extended to include the elastic errors, by explicitly considering the task loading and payload weight dependency of the errors. This is done by incorporating a method called GEC, which has been developed to identify the elastic errors as a function of the manipulator's configuration and task loading wrenches at the end-effector (Meggiolaro et al., 1998).

Results presented here show that the location selected for endpoint contact significantly affects SEC calibration performance. A technique to find the optimal calibration point is presented with simulation results.

Also, to use the method for applications without significant task loads, it is necessary to minimize the forces between the manipulator and the calibration point fixture. Large forces could result in significant elastic deformations on the SEC fixture and the manipulator, compromising the identification accuracy. This paper shows how to keep endpoint forces small while moving a manipulator under endpoint constraint.

The calibration method is applied experimentally to a 6 DOF hydraulic manipulator. The error parameters of the robot are identified and used to predict, and compensate for, the endpoint errors as a function of configuration. These experimental results show that the method is able to effectively and significantly improve the manipulator's accuracy without requiring special and expensive metrology equipment.

ANALYTICAL BACKGROUND

Model Based Error Compensation

The distortion of a manipulator from its ideal shape due to such factors as manufacturing errors results in the reference frames that define the manipulator joints being slightly displaced from their expected, ideal locations. This creates significant end-effector errors when the manipulator's ideal model is used to predict its performance. The position and orientation of a manipulator's frame F_i^{real} with respect to its ideal location F_i^{ideal} is represented by a 4x4 homogeneous matrix E_i , see Figure 1. The translational part of matrix E_i is composed of 3 coordinates, and the rotational part of matrix E_i is the result of the product of three consecutive rotations. These 6 parameters are called generalized error parameters, which can be a function of the system geometry and joint variables (Everett and Suryohadiprojo, 1988). For an n degree of freedom manipulator, there are 6(n+1) generalized errors. These can be represented in vector form as a 6(n+1) x 1 vector, called ϵ , assuming that both the manipulator and the location of its base are being calibrated. If only the manipulator is being calibrated, then the number of generalized errors is 6n.

The end-effector position and orientation error ΔX is defined as the 6x1 vector that represents the difference between the real position and orientation of the end-effector and the ideal one:

$$\Delta X = X^{real} - X^{ideal} \quad (1)$$

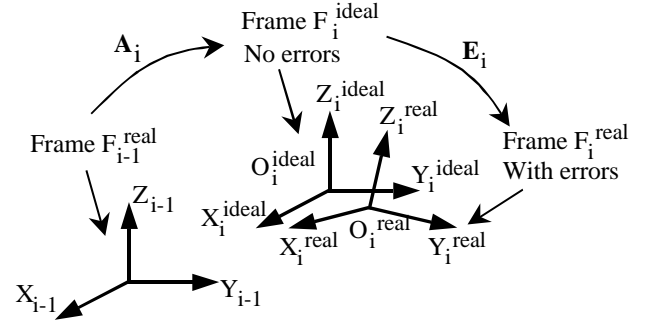


Figure 1. Frame Translation and Rotation Due to Errors for i^{th} Link

where X^{real} and X^{ideal} are the 6x1 vectors composed of the three positions and three orientations of the end-effector reference frame in the inertial reference system for the real and ideal cases, respectively. Since the generalized errors are small, ΔX can be calculated using the linear equation in ϵ :

$$\Delta X = J_e \epsilon \quad (2)$$

where J_e is the 6x6(n+1) Jacobian matrix of the end-effector error ΔX with respect to the elements of the generalized error vector ϵ , also known as Identification Jacobian matrix (Zhuang et al., 1999). If the generalized errors, ϵ , can be found from calibration measurements, then the correct end-effector position and orientation error can be calculated using Equation (2) and be compensated. The method to obtain ϵ from experimental measurements is explained below.

Identification of the Generalized Errors

The identification of the 6(n+1) components of generalized errors ϵ for an n DOF manipulator is based on measuring the components of the end-effector error vector ΔX at a finite number (m) of different manipulator configurations. The m configurations are represented by m vectors of joint variables, q_1, q_2, \dots, q_m . Equation (2) can be written m times:

$$\Delta X_t = \begin{bmatrix} \Delta X_1 \\ \Delta X_2 \\ \dots \\ \Delta X_m \end{bmatrix} = \begin{bmatrix} J_e(q_1) \\ J_e(q_2) \\ \dots \\ J_e(q_m) \end{bmatrix} \cdot \epsilon = J_t \cdot \epsilon \quad (3)$$

where ΔX_t is the m x 1 vector formed by all measured vectors ΔX at the m different configurations and J_t is the 6m x 6(n+1) Total Identification Jacobian matrix. The matrix J_t is formed from the m Identification Jacobian matrices J_e at the m configurations. To compensate for the effects of measurement noise, the number of measurements m is in general much larger than n.

In practice, the position coordinates of ΔX are easier to measure than the orientations, so often only the three position coordinates of ΔX are measured. In this case, twice the number

of measurements is required to obtain the same calibration accuracy.

If the generalized errors are constant, then a unique least-squares estimate $\hat{\boldsymbol{\epsilon}}$ can be calculated by (Roth et al., 1987):

$$\hat{\boldsymbol{\epsilon}} = (\mathbf{J}_t^T \mathbf{J}_t)^{-1} \mathbf{J}_t^T \cdot \Delta \mathbf{X}_t \quad (4)$$

If the Identification Jacobian matrix $\mathbf{J}_e(\mathbf{q}_i)$ contains linear dependent columns, then Equation (4) will give estimates with poor accuracy. This occurs when there is redundancy in the error model, in which case it is not possible to distinguish the amount of the error contributed by each generalized error ϵ_{ij} . To eliminate this problem, the columns of \mathbf{J}_e must be reduced to a linear independent set. This reduction can be performed analytically by using the equations presented in (Meggiolaro and Dubowsky, 2000). The generalized errors are then grouped into a smaller independent set, resulting in identification with improved accuracy.

However, most manipulator calibration techniques to obtain the measurements in Equation (3) require expensive and/or complicated pose measuring devices, such as theodolites. Thus the current interest in closed-loop methods that do not require such equipment. The SEC closed-loop calibration method, which uses data only from the internal sensors of a robot, is described below.

SINGLE ENDPOINT CONTACT (SEC) CALIBRATION

In Single Endpoint Contact calibration, instead of moving the end-effector to different positions to obtain the calibration measurements in Equation (3), the endpoint position is kept fixed with changes only in its orientation. This is equivalent to grasping a ball joint, resulting in three calibration equations per pose. The advantage of this method is that it does not require measurements of the robot position using external sensors, requiring only an inexpensive and compact device such as a ball joint. Only one endpoint needs to be known and the joint angle measurements. The kinematic loop closure equations are enough to calibrate the manipulator from joint readings alone. In order to calibrate the system, the closed chain must have some mobility. So, a spatial manipulator must have 4 DOF's or more to be calibrated using this method. For planar manipulators, the point contact condition provides 2 constraints, so a planar manipulator with as few as 3 DOF's may be calibrated using SEC.

Analytical Development

Consider the manipulator gripping the end-effector fixture at a constant location (x_0, y_0, z_0) , and define \mathbf{q}^{real} as the measured vector of joint variables. The end-effector error is the difference between the actual position of the end-effector, at the SEC fixture, and the ideal position calculated from the ideal kinematic equations applied to the measured \mathbf{q}^{real} . This ideal position is the end-effector position that an ideal manipulator would achieve if it was moved to the measured joint readings

of the actual robot. As both ideal and real manipulator positions are evaluated at the same configuration \mathbf{q}^{real} , the resulting end-effector error $\Delta \mathbf{X}$ is only due to the generalized errors. From Equations (1-2), the end-effector position error $\Delta \mathbf{X}$ is

$$\Delta \mathbf{X} = \mathbf{X}^{\text{real}}(\mathbf{q}^{\text{real}}) - \mathbf{X}^{\text{ideal}}(\mathbf{q}^{\text{real}}) = [x_0, y_0, z_0]^T - \mathbf{X}^{\text{ideal}} = \mathbf{J}_e(\mathbf{q}^{\text{real}}) \boldsymbol{\epsilon} \quad (5)$$

Here the three end-effector reference frame orientations are eliminated from the error model, as they are not measured. The three position components of the end-effector reference frame in the inertial reference system are represented by the 3x1 endpoint vectors \mathbf{X}^{real} and $\mathbf{X}^{\text{ideal}}$.

Since both \mathbf{J}_e and $\mathbf{X}^{\text{ideal}}$ can be calculated at each point using the measured joint positions and ideal direct kinematics, the only remaining unknown in Equation (5) is the generalized error vector $\boldsymbol{\epsilon}$.

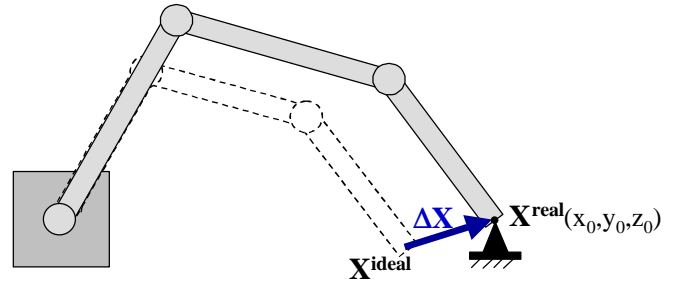


Figure 2. Real and Ideal Positions of a Manipulator End-Effector

So, as the robot executes self-motions to different configurations, the real robot parameters can be estimated from the readings of the internal position sensors and from the identification model. A total least squares optimization procedure, shown in Equation (4), is then used to improve the calibration accuracy.

As in every calibration not having *a priori* knowledge of the task constraint dimensions, the scale of the mechanism must be set, i.e., one link length or other length parameter has to be measured by independent means (Bennett and Hollerbach, 1991). In the SEC method, if any of the coordinates x_0 , y_0 or z_0 of the end-effector fixture is known, then this scaling requirement is already satisfied. However, if none of these coordinates is known, then one length parameter needs to be independently measured. Note that it is not necessary to know *a priori* the location of the end-effector fixture, since its location can be introduced as an unknown. In this case, Equation (5) is rewritten as

$$-\mathbf{X}^{\text{ideal}} = \begin{bmatrix} \mathbf{J}_e & \begin{bmatrix} -1 & 0 & 0 \\ 0 & -1 & 0 \\ 0 & 0 & -1 \end{bmatrix} \end{bmatrix} \cdot \begin{bmatrix} \boldsymbol{\epsilon} \\ x_0 \\ y_0 \\ z_0 \end{bmatrix} = \mathbf{J}_e^* \boldsymbol{\epsilon}^* \quad (6)$$

where the unknown vector $\boldsymbol{\varepsilon}^*$ contains both generalized errors and the coordinates of the end-effector fixture.

In addition to geometric errors, this calibration method is able to identify elastic structural deformation errors, since arbitrary forces can be applied to the SEC fixture. In this case, an extended error model must be used to identify the elastic errors as a function of the payload wrench at the end-effector, as discussed before. Defining \mathbf{F} as the desired force applied to the end-effector and \mathbf{J} as the robot Jacobian, then the vector $\boldsymbol{\tau}$ of applied joint torques/forces to the manipulator is

$$\boldsymbol{\tau} = \mathbf{J}^T (-\mathbf{F}) \quad (7)$$

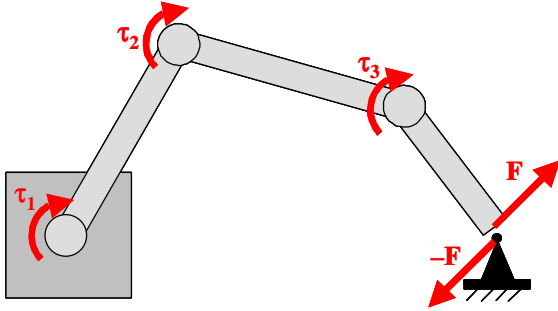


Figure 3. Calibration of Elastic Errors due to an Arbitrary Force

Control

To use the SEC method, the manipulator must be controlled to move the joint variables while keeping the end-effector still. To accomplish this without causing large and unknown forces on the end-effector that would deform the SEC fixture or the manipulator, a projection approach is adopted. In the method the control input is a projected error proportional feedback of the form:

$$\mathbf{u} = (\mathbf{I} - \mathbf{J}^\# \cdot \mathbf{J}) \cdot [\mathbf{K} \cdot (\mathbf{q}_r - \mathbf{q})] \quad (8)$$

where \mathbf{J} is the robot Jacobian, $\mathbf{J}^\#$ is the Jacobian pseudoinverse, \mathbf{K} is a positive definite matrix, and \mathbf{q}_r is the desired manipulator configuration. The matrix $(\mathbf{I} - \mathbf{J}^\# \cdot \mathbf{J})$ is the orthogonal projection operator in the Jacobian null space, which guarantees that joint velocities do not result in any end-effector velocity. Note that the above control scheme is equivalent to using the

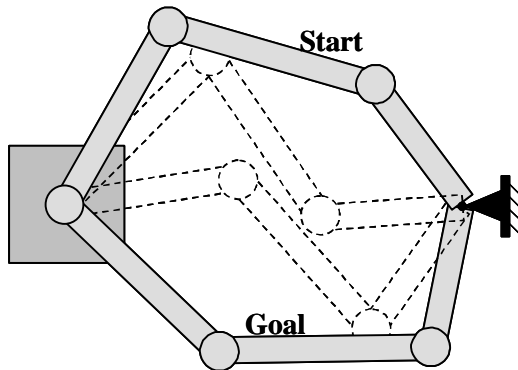


Figure 4. Stabilization of the Arm Self-Motions

classical Projected Gradient method (Oriolo, 1994) to solve redundancy. It has been shown that the reference configuration \mathbf{q}_r is globally stable for this control scheme. Thus, this control approach is used to steer the manipulator into different configurations.

OPTIMIZATION OF THE FIXTURE LOCATION

In SEC calibration, the location of the endpoint device can significantly affect the calibration performance. Ideally, the generalized errors are constant in their frames, and the errors identified at an arbitrary configuration can be used to compensate the errors at any other configuration. In this case, the chosen location used by the SEC does not influence the calibration accuracy, since any configuration would lead to the same constant generalized errors. However, the generalized errors are in general functions of the configuration, especially in systems with significant elastic deformation. Therefore, interpolating functions must be chosen to model each generalized error, and its coefficients must be identified (Meggiolaro et al., 1998).

Furthermore, depending on the chosen set of measurement points, the error compensation process involves interpolation or extrapolation of the generalized error functions. As a general mathematical result, the interpolation accuracy can be improved to the limit of the measurement noise by performing enough measurements in the desired range. But the extrapolation accuracy depends on the chosen set of functions, especially on how well they model the actual system. So, poorly chosen functions may give a reasonable precision in the interpolation range, but its accuracy is compromised in configurations outside the measured range. As a result, the choice of the measurement ranges at each joint is critical to the calibration accuracy.

In the SEC calibration, the measurement ranges of each joint are uniquely defined by the location of the calibration point. For a generic manipulator, it is necessary to use numerical methods to find the measurement ranges. If the manipulator inverse kinematic equations can be written, then it is possible to find analytical solutions for the joint ranges. For an ideal 3R planar manipulator, with full-range of all 3 joints and no interference between links, an analytical solution of the measurement ranges for each calibration point P has been found, as given below.

Defining l_i as the length of link i and $\mathbf{P} = [r \cos \varphi, r \sin \varphi]$ as the calibration point, the joint angles q_i must satisfy:

$$\begin{aligned} k_{11} &\equiv \frac{r^2 + l_1^2 - (l_2 + l_3)^2}{2l_1 r} \leq \cos(q_1 - \varphi) \leq \frac{r^2 + l_1^2 - (l_2 - l_3)^2}{2l_1 r} \equiv k_{12} \\ k_{21} &\equiv \frac{(r - l_3)^2 - l_1^2 - l_2^2}{2l_1 l_2} \leq \cos(q_2) \leq \frac{(r + l_3)^2 - l_1^2 - l_2^2}{2l_1 l_2} \equiv k_{22} \\ k_{31} &\equiv \frac{(r - l_1)^2 - l_2^2 - l_3^2}{2l_2 l_3} \leq \cos(q_3) \leq \frac{(r + l_1)^2 - l_2^2 - l_3^2}{2l_2 l_3} \equiv k_{32} \quad (9) \end{aligned}$$

The calibrated range of a joint j can then be written as:

$$q_j \in [q_{j0} - q_{j1}, q_{j0} - q_{j2}] \cup [q_{j0} + q_{j2}, q_{j0} + q_{j1}] \quad (10)$$

where

$$q_{ji} \equiv \begin{cases} \delta & \text{if } k_{ji} \leq -1 \\ 0 & \text{if } k_{ji} \geq 1 \\ \text{acos}(k_{ji}) & \text{if } -1 \leq k_{ji} \leq 1 \end{cases} \quad \text{and} \quad q_{j0} \equiv \begin{cases} \varphi & \text{if } j = 1 \\ 0 & \text{if } j = 2 \\ 0 & \text{if } j = 3 \end{cases} \quad (11)$$

For a generic 3R manipulator, it is also necessary to consider the intersection between the ideal solution from Equation (10) and the mechanical limits of each joint.

Once the measurement ranges of each joint are calculated and the errors identified using SEC, the calibration performance can be evaluated by defining a performance index. This index is based on the idea that measurement interpolation results in better accuracy than extrapolation. First consider the Interpolated Compensation Region (ICR), defined as the region of the workspace where the compensation algorithm does not require extrapolation of the error functions. It represents the region of the workspace that the manipulator can reach by independently sweeping its joints through their interpolated ranges. Conversely, the Extrapolated Compensation Region (ECR) is the workspace region where any of the generalized error functions needs to be extrapolated, resulting in reduced accuracy.

In order to obtain an ideal location of the calibration point, a performance index for the SEC method needs to be defined and optimized. The volume of the ICR is an example of such index. As a calibration point P is chosen to maximize this volume - therefore minimizing the volume of the ECR - the overall accuracy of the compensation algorithm is increased. But in this way, every region of the workspace is given the same importance, even those that are not useful for the task to be performed after calibration. To choose the fixture location that offers the best accuracy in specific workspace regions, a more general index is defined, called the Weighted Volume of the ICR (WV):

$$WV = \iiint_{ICR} \alpha(x, y, z) \cdot dV \quad (12)$$

where $\alpha(x,y,z) \in [0,1]$ is a weight function defined in the whole workspace, representing the importance of each point (x,y,z) on the chosen task. Note that if $\alpha(x,y,z)=1$ in the whole workspace, then the WV becomes the geometric volume of the ICR. The choice of the best fixture location for the SEC method is obtained by maximizing the function WV.

RESULTS

Simulations of the SEC calibration and the optimization of the fixture location were performed for two 3R planar

manipulators and a 6-DOF manipulator. Experiments were then performed on a Schilling Titan II manipulator to show the effectiveness of the SEC calibration.

Simulation Results

Two different 3R planar manipulators were considered, with link lengths $(1, 1, 1)$ and $(5, 4, 3)$. In both cases an optimal location of the SEC fixture was found. For the $(1, 1, 1)$ manipulator, the location that maximizes the volume of the interpolated region is at a distance from the robot base equal to 1.0 (see Figure 5). By using this fixture location, it is possible to move the manipulator in the full-range of its 3 joints, and the errors along the entire workspace can be compensated without extrapolation. Note that in this example the considered weights $\alpha(x,y,z)$ of the Weighted Volume are equal to 1.0, i.e., every region of the workspace is considered equally important.

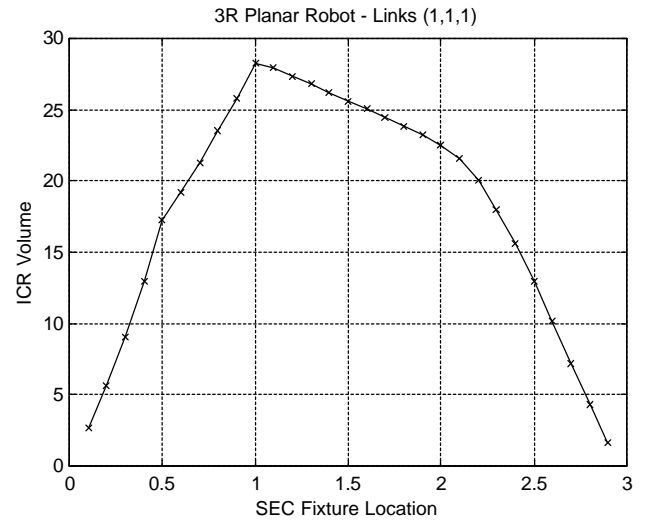


Figure 5. ICR Volume as a Function of the Fixture Location

For the $(5, 4, 3)$ planar manipulator, the optimal solution of the fixture location is at a distance from the robot base equal to 6.0 (see Figure 6). In this case, however, the ICR is not coincident with the workspace. The maximum volume (or area, since it's a planar manipulator) of the ICR is 341.6, while the workspace surface is $\pi \cdot 12^2 = 452.4$. So, even for the best choice of the calibration point, still 25% of the calibrated workspace relies on extrapolation to compensate for the measured errors. Figure 7 shows some of the 3R manipulator configurations corresponding to a fixture location at $P(x,y)=(6,0)$. The Interpolated and Extrapolated Compensation Regions obtained after the calibration process at two different fixture locations are shown in Figures 8 and 9. Note that the ICR obtained from calibration at the optimal fixture location $P=(6,0)$, shown in Figure 8, is much larger than the one obtained using $P=(10,0)$. Thus it is expected that the SEC calibration at $P=(6,0)$ results in better accuracy than using a fixture location at $P=(10,0)$.

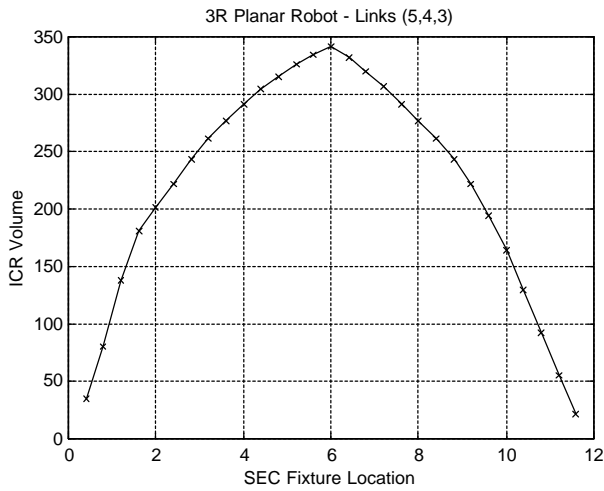


Figure 6. ICR Volume as a Function of the Fixture Location

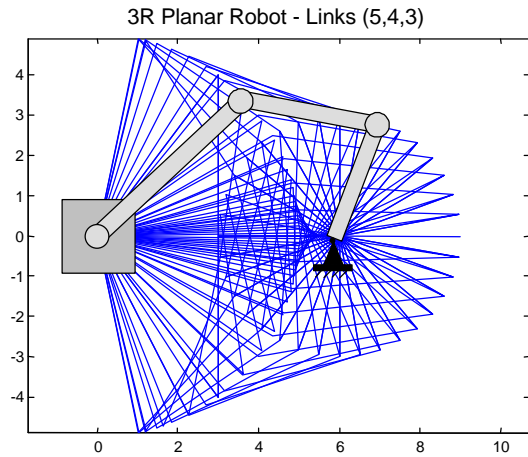


Figure 7. Measurement Configurations for an SEC Fixture Located at (6,0)

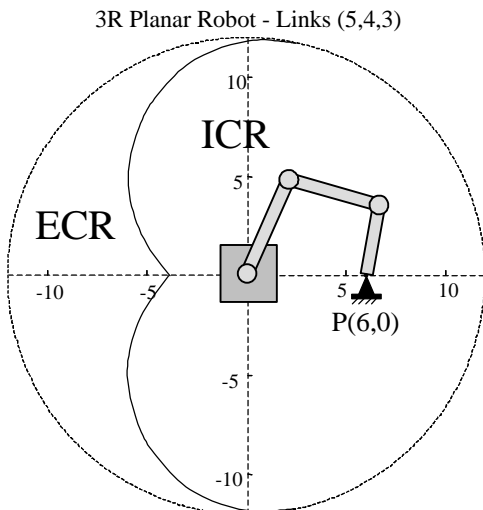


Figure 8. Extrapolated and Interpolated Compensation Regions for an SEC Fixture at (6,0)

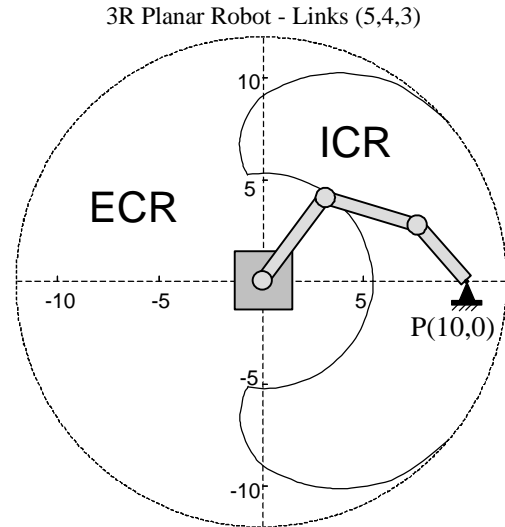


Figure 9. Extrapolated and Interpolated Compensation Regions for an SEC Fixture at (10,0)

A simulation of the SEC method was applied to a 3R planar manipulator with link lengths (1m, 1m, 1m). The simulation introduced generalized errors that are not constant in their reference frames, reflecting the effects of elastic deformations. To investigate the effects of interpolation and extrapolation on the measured errors, the chosen identification functions were different from the introduced error functions, otherwise the simulation would always result in a perfect fit.

Two different fixture locations are used in the calibration, at distances 1.0m (the optimal location in this case) and 2.5m from the manipulator base. The manipulator is moved to several measurement configurations, sweeping the joint ranges allowed by each fixture location. An RMS uncorrected error of 8.0mm and a measurement noise of 0.1mm were introduced to both simulations. After the identification process, the end-effector was released and the compensated manipulator was moved to all possible configurations in the workspace. The residual error after compensation was then evaluated at each configuration, and its RMS value was calculated.

For the calibration fixture at 1.0m, the full range of the three joints was achieved, and the RMS residual error was 0.16mm. When the fixture location was changed to 2.5m from the robot base, the RMS residual error was 0.49mm, approximately 3 times higher. This poorer accuracy is mainly due to the measurement range of joint 1 being restricted to the interval $[-49^\circ, 49^\circ]$, therefore all configurations outside this range are compensated using extrapolations. Unless the chosen interpolation functions perfectly model the generalized errors, the SEC fixture location plays a critical role on the calibration accuracy.

Figure 10 shows the RMS residual error for the (1m, 1m, 1m) planar manipulator as a function of the number of measurement points, for different measurement noise levels. Note that calibration cannot be made infinitely accurate as the number of measurement points is increased, and a lower bound

exists on the calibration error that is dictated by robot repeatability and calibration measurement error (Roth et al., 1987). This is captured by the graph in Figure 9, showing residual errors tending to the measurement noise levels as the number of points is increased.

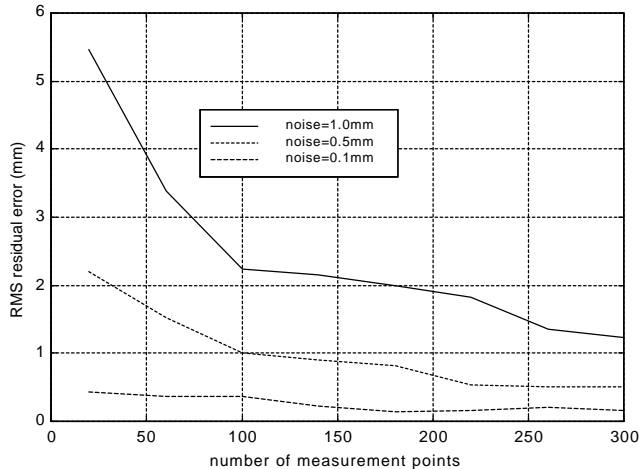


Figure 10. RMS Residual Error as a Function of the Number of Measurements

Simulations were also performed for a Schilling Titan II manipulator, a 6-DOF hydraulic robot. Using these results the SEC performance was analyzed for two different calibration device lengths: 10 and 50 inches (254 and 1270mm). These lengths are the distance between the device gripper, attached to the robot end-effector, and the center of rotation of the spherical joint. The device length plays an important role on the achievable measurement ranges, since it modifies the loop closure equations.

Due to the rotational symmetry of the system around joint 1, the optimal location of the calibration device is on the vertical plane defined by the middle of the mechanical limits of joint 1. The optimal location for the 254mm device is calculated at $P(x, z) = (550\text{mm}, 1800\text{mm})$, respectively the horizontal and vertical distances from the manipulator base along the defined vertical plane. The volume of the ICR in this case is 8.33m^3 . A second maxima for the ICR volume is 6.66m^3 , obtained for a device location at $P(x, z) = (550\text{mm}, -200\text{mm})$ from the manipulator base. For the 1270mm device, the optimized location is at $P(x, z) = (1600\text{mm}, 1750\text{mm})$, resulting in an ICR volume of 17.8m^3 . Note that this volume is twice the ICR volume obtained from the 254mm device, i.e., the 1270mm fixture results in a better calibration accuracy in this case.

Experimental Results

Figure 11 shows the laboratory system used to experimentally evaluate the SEC calibration method. The manipulator is a Schilling Titan II, a six DOF hydraulic robot capable of handling payloads in excess of 100 kg. A handle on the SEC fixture provides a repeatable grip for the manipulator.

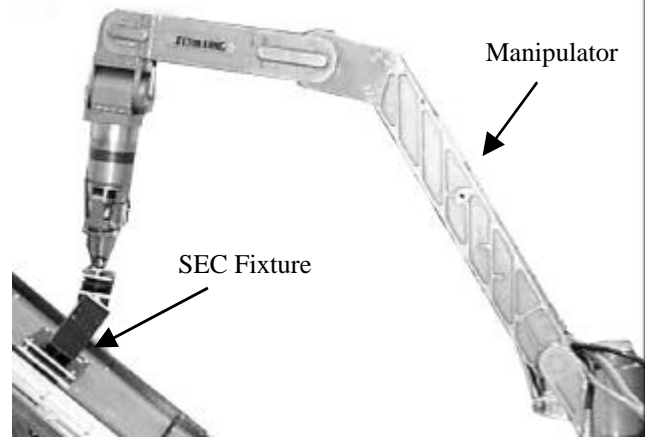


Figure 11. Experimental System

The objective of the experiment is to see if the SEC calibration method can be practically applied to a real physical system to improve its absolute accuracy. The object is to have the residual error approach the limit set by the position sensing resolution of the system. A control technique called Base Sensor Control (Iagnemma et al., 1997) is used to improve the system repeatability by greatly reducing the effects of joint friction. This control scheme is applied in concert with the orthogonal projection operator in the Jacobian null space, defined in Equation (8), minimizing the resulting forces at the SEC fixture. The relative positioning root mean square error is used as a measure of the system repeatability. Data is taken by moving the manipulator an arbitrary distance from the test point and then commanding it back to its original position. The measured maximum errors are ± 5 mm, and the repeatability of the system is 2.7 mm (RMS).

Although the Base Sensor Control algorithm greatly reduces the repeatability errors, there are still 45mm (RMS) errors in absolute accuracy. Since the system repeatability is relatively small with respect to the absolute errors, a model based error compensation method can be applied to reduce the accuracy errors, such as the SEC method.

In order to implement SEC, the generalized error functions were interpolated using approximately 800 measurements of the robot configuration. These measurements were performed for an SEC device with length 155mm located at $P(x, z) = (1440\text{mm}, 265\text{mm})$ from the manipulator base. Note that the end-effector fixture location was obtained by the SEC calibration, since it was not known *a priori*. After the identification process, the compensated manipulator was moved to 200 different configurations to verify the efficiency of the SEC method.

Figure 12 shows the convergence of original positioning errors as large as 98.5mm (44.8mm RMS) to corrected absolute errors of less than 15mm (5.7mm RMS) with respect to the base frame. This demonstrates an overall factor of nearly 8 improvement in absolute accuracy by using the SEC calibration algorithm. This improvement in performance shows that such calibration method is able to effectively identify and correct for the errors in the system.

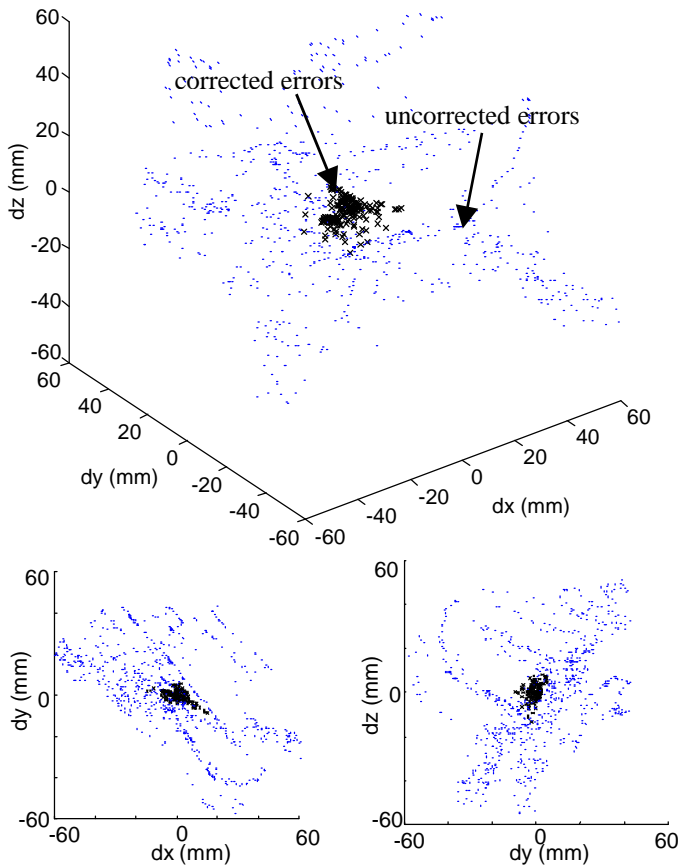


Figure 12. Measured and Residual Errors After Compensation

CONCLUSIONS

In this paper, a calibration method that does not require endpoint measurements or precision points has been investigated. The method constrains the robot end-effector to a fixture equivalent to a spherical joint. The required fixture has the advantage of being inexpensive and compact when compared to pose measuring devices required by other calibration techniques. By forming the manipulator into a mobile closed kinematic chain, the kinematic loop closure equations are adequate to calibrate the manipulator from joint readings alone. A performance index is introduced to calculate the optimal location of the calibration device. The method is evaluated experimentally on a Schilling Titan II manipulator. The results show that the calibration method is able to effectively identify and correct for the errors in the system.

ACKNOWLEDGMENTS

The support of the Korean Electric Power Research Institute (KEPRI), Electricité de France (EDF), and the Brazilian government (through CAPES) in this research is appreciated.

REFERENCES

- Abdel-Malek, K. and Yeh, H.J., 1997, "Analytical Boundary of the Workspace for General 3-DOF Mechanisms", *The International Journal of Robotics Research*, vol. 16, no. 2, April 1997, pp. 198-213.
- Bennett, D.J. and Hollerbach, J.M., 1991, "Autonomous Calibration of Single-Loop Closed Kinematic Chains Formed by Manipulators with Passive Endpoint Constraints", *IEEE Trans. Robotics & Automation*, Vol. 7, No. 5, pp.597-606.
- Burdick, J.W., 1989, "On the Inverse Kinematics of Redundant Manipulators: Characterization of the Self-Motion Manifolds", *Proceedings of the IEEE International Conference on Robotics and Automation*, May 14-19, pp. 264-270. vol.1
- Everett, L.J., Lin, C.Y., 1988, "Kinematic Calibration of Manipulators with Closed Loop Actuated Joints," *Proc. IEEE International Conf. On Robotics and Automation*, Philadelphia, pp.792-797.
- Everett, L.J., Suryodiprjo, A.H., 1988, "A Study of Kinematic Models for Forward Calibration of Manipulators," *Proc. IEEE International Conf. On Robotics and Automation*, Philadelphia, pp.798-800.
- Hayati, S.A., 1983, "Robot Arm Geometry Link Parameter Estimation," *Proc. 22nd IEEE Conference Decision and Control*, San Antonio, pp.1477-1483.
- Hollerbach, J., 1988, "A Survey of Kinematic Calibration," *Robotics Review*, Khatib et al ed., Cambridge, MA, MIT Press.
- Hollerbach, J.M., Wampler, C.W., 1996, "The Calibration Index and Taxonomy for Robot Kinematic Calibration Methods," *Int. J. of Robotics Research*, **15**(6): pp.573-591.
- Hsu, T.-W., Everett, L.J., 1985, "Identification of the Kinematic Parameters of a Robot Manipulator for Positional Accuracy Improvement," *Proc. Computers in Engineering Conference*, Boston, pp.263-267.
- Huang, Q., 1984, "Study on the Workspace of a R-Robot", Publ. by SME, Dearborn, MI, *Robots 8, Conference Proceedings*, Detroit, MI, vol. 1, pp. 4.55-4.66.
- Iagnemma, K., Morel, G. and Dubowsky, S., 1997, "A Model-Free Fine Position Control System Using the Base-Sensor: With Application to a Hydraulic Manipulator." *Symposium on Robot Control, SYROCO '97*, **2**, pp. 359-365.
- Ikits, M., Hollerbach, J.M., 1997, "Kinematic Calibration Using a Plane Constraint," *IEEE International Conference on Robotics and Automation*, Albuquerque, New Mexico, pp. 3191-3196.
- Meggiolaro, M., Mavroidis, C. and Dubowsky, S., 1998, "Identification and Compensation of Geometric and Elastic Errors in Large Manipulators: Application to a High Accuracy Medical Robot." *Proceedings of the 1998 ASME Design Engineering Technical Conference*, Atlanta.

Meggiolaro, M. and Dubowsky, S., 2000, "An Analytical Method to Eliminate the Redundant Parameters in Robot Calibration," *Proc. of IEEE Int. Conference on Robotics and Automation (ICRA 2000)*, pp. 3609-3615, Stanford, CA

Oriolo, G., 1994, "Stabilization of Self-Motions in Redundant Robots", *Proceedings of the IEEE International Conference on Robotics and Automation*, pp. 704-709.

Ottaviano, E., Ceccarelli, M. and Lanni, C., 1999, "A Characterization of Ring Void in Workspace of Three-Revolute Manipulators", *Proc. of the 10th World Congress on the Theory of Machines and Mechanisms*, pp. 1039-1044, Oulu, Finland

Roth, B., 1976, "Performance Evaluation of Manipulators from a Kinematic Viewpoint", *Performance Evaluation of Programmable Robots and Manipulators*, National Bureau of Standards, Special Publ. 459, pp. 39-61.

Roth, Z.S., Mooring, B.W., Ravani, B., 1987, "An Overview of Robot Calibration," *IEEE Journal of Robotics and Automation*, 3(5): pp.377-384.

Schröer, K., 1993, Theory of Kinematic Modeling and Numerical Procedures for Robot Calibration. In Bernhardt, R., Albright, S.L. (eds.): *Robot Calibration*. London: Chapman & Hall, pp.157-196.

Yang, D.C.H. and Lee, T.W., 1983, "On the Workspace of Mechanical Manipulators", *Transactions of the ASME, Journal of Mechanical Design*, vol. 105, pp. 62-69.

Zhuang, H., 1997, "Self Calibration of Parallel Mechanisms with a Case Study on Stewart Platforms", *IEEE Trans. Robotics & Automation*, Vol. 13, No. 3, June 1997, pp.387-397.

Zhuang, H., Motaghedi, S.H., Roth, Z.S., 1999, "Robot Calibration with Planar Constraints," *Proc. IEEE International Conference of Robotics and Automation*, Detroit, Michigan, pp.805-810.

Ziegert, J., Datseris, P., 1988, "Basic Considerations for Robot Calibration," *Proc. IEEE International Conference on Robotics and Automation*, Philadelphia, pp.932-938.